

Short Communication

## Fabrication of $\text{LiNi}_{0.8}\text{Co}_{0.1}\text{Mn}_{0.1}\text{O}_2$ cathode materials via Sodium Dodecyl Benzene Sulfonate-assisted hydrothermal Synthesis for Lithium Ion Batteries

Chuanning Yang<sup>1,2,3,\*</sup>, Wangchuan Xiao<sup>1,3</sup>, Shizhao Ren<sup>1</sup>, Qiyong Li<sup>1</sup>, Jianhua Wang<sup>1</sup>, Zhuolin Li<sup>1</sup>, Wanting Li<sup>1</sup>, Bingxin Chen<sup>1</sup>

<sup>1</sup> School of Resource and Chemical Engineering, Sanming University, Sanming, Fujian 365004, China

<sup>2</sup> Science and Technology, Sanming Institute of the Fluorochemical Industry, Sanming, Fujian 365004, China

<sup>3</sup> Fujian Fluorine Based Chemical Engineering Service Platform of Science and Technology Combined with Economy, Sanming University, Sanming Fujian 365004, China

\*E-mail: [yensuper@163.com](mailto:yensuper@163.com)

Received: 24 October 2022 / Accepted: 1 December 2022 / Published: 27 December 2022

The ternary cathode material  $\text{LiNi}_{0.8}\text{Co}_{0.1}\text{Mn}_{0.1}\text{O}_2$  for lithium ion batteries was prepared by a novel route by adding sodium dodecyl benzene sulfonate (LAS) which is a surfactant can greatly alleviate the serious agglomeration of particles of the products. The ternary cathode materials were synthesized with metal sulfate as raw materials by the method of hydroxyl co-precipitation. The samples were characterized by XRD, SEM, and electrochemical tests. The mechanism of LAS was analyzed also. The results show that the morphology of acquired particles with 0.42g-LAS was more regular and uniform than that without LAS. The structure of the acquired materials were not affected by adding LAS. The specific capacity of charge and discharge was 240.2 mAh/g, 189.5 mAh/g, and the coulombic efficiency was 78.9% higher than other samples. The specific discharge capacity is 186.3 mAh/g after 50 cycles.

**Keywords:** sodium dodecyl benzene sulfonate; NCM 811 cathode; composite material; nanostructure; lithium ion batteries

### 1. INTRODUCTION

Owing to the increasing requirements for energy storage devices based on lithium ion batteries (LIBs) have been used as the green power sources which have drawn tremendous attentions of the new electrochemical energy storage community [1-5]. Recently, the ternary cathode materials ( $\text{LiNi}_x\text{Co}_y\text{Mn}_z\text{O}_2$ ), with a layered structure, has become an immediate area of research focus due to its excellent electrochemical performance. Especially for the ternary cathode materials of

$\text{LiNi}_{0.8}\text{Co}_{0.1}\text{Mn}_{0.1}\text{O}_2$  as the nickel-rich ternary materials which have considerably high specific capacity [6-9].

However, the widespread application of  $\text{LiNi}_{0.8}\text{Co}_{0.1}\text{Mn}_{0.1}\text{O}_2$  ternary cathode materials still has enormous challenge, including long-term cyclic stability which correlate with cation mixing in the bulk structure. The cation mixing will lead to lithium ion deintercalation, which will weaken the diffusion ability of lithium ion and reduce the electrochemical performance [10-15]. With the increase of nickel content, the cation disorder is aggravated, and the stability, cycle and life of the material are reduced.

The  $\text{LiNi}_{0.8}\text{Co}_{0.1}\text{Mn}_{0.1}\text{O}_2$  ternary cathode ternary materials prepared by hydroxyl co-precipitation method have the advantages of high vibration density, good machining performance and easy morphology control, so it has become the mainstream research and development direction of industrialization at present [16-18]. The study show that the surfactant in the solution has a certain adsorption effect on the product particles [19-21]. It mainly includes physical adsorption and chemical adsorption. Physical adsorption includes the following ways: ion exchange adsorption, ion pair adsorption, hydrogen bond adsorption,  $\pi$  electron polarization adsorption, hydrophobic adsorption [22-25]. In the category of chemisorption, the reactive group of the surfactant forms a new chemical bond with the surface group of the precursor particle, thus achieving the modification and modification of the surface [26-29].

Herein, we introduce the sodium dodecyl benzene sulfonate (LAS) as the surfactant additive which can alleviate the severe agglomeration of precursor particles caused by excessive alkali concentration in traditional hydroxyl co-precipitation process during the fabrication of  $\text{LiNi}_{0.8}\text{Co}_{0.1}\text{Mn}_{0.1}\text{O}_2$ . Meanwhile, the composite with layered nanostructure shows excellent electrochemical performance as the cathode for lithium ion batteries.

## 2. MATERIALS AND METHODS

### 2.1 Materials Preparation

For the fabrication of materials, the  $\text{LiNi}_{0.8}\text{Co}_{0.1}\text{Mn}_{0.1}\text{O}_2$  ternary cathode materials were fabricated by as follows; An aqueous solution of  $\text{NiSO}_4 \cdot 6\text{H}_2\text{O}$  (Sigma-Aldrich, AG, China),  $\text{CoSO}_4 \cdot \text{H}_2\text{O}$  (Sigma-Aldrich, AG, China) and  $\text{MnSO}_4 \cdot \text{H}_2\text{O}$  (Sigma-Aldrich, AG, China) (cationic ratio of Ni:Co:Mn = 8:1:1) with a concentration of 2.0 mol/mL, and then pumped into continuous stirred tank reactor (CSTR, capacity 4 L) under nitrogen atmosphere. Meanwhile, NaOH solution (Sigma-Aldrich, AG, China) solution of 2.0 mol/mL as the precipitant with adding a certain concentration of sodium dodecyl benzene sulfonate (LAS) (Sigma-Aldrich, AG, China) solution and desired amount of  $\text{NH}_4\text{OH}$  solution (Sigma-Aldrich, AG, China) as a chelating agent were also separately fed into the reactor. The additive amounts of LAS were 0.0g, 0.21 g, 0.42g and 0.63g, respectively. The concentration of LAS were 0.0 mol/mL, 0.1 mol/mL, 0.2 mol/mL and 0.3 mol/mL, respectively. The concentration of the solution, pH, temperature, and the speed of the mixture in the reactor were controlled precisely. Especially, to make sure the acid-base environment of co-precipitation, the pH

should be about 10.5. At the initial stage of the hydroxyl co-precipitation process, the irregular secondary particles changed gradually into spherical particles by vigorous stirring under the speed of 600 r/min at 60 °C for 12 h. Then, the finally acquired spherical  $\text{Ni}_{0.8}\text{Co}_{0.1}\text{Mn}_{0.1}(\text{OH})_2$  particles were collected and washed with DIW and ethanol several times, following by vacuum drying at 110 °C overnight.

The acquired  $\text{Ni}_{0.8}\text{Co}_{0.1}\text{Mn}_{0.1}(\text{OH})_2$  particles were mixed with  $\text{LiOH}\cdot\text{H}_2\text{O}$  powders thoroughly. The mixture was first heated at 400 °C for 5h in air, and it was calcined at 900 °C for 15 h in air to obtain  $\text{LiNi}_{0.8}\text{Co}_{0.1}\text{Mn}_{0.1}\text{O}_2$  ternary cathode composite materials which were named LAS-1 and LAS-2, LAS-3, LAS-4 according to the additive amount of sodium dodecyl benzene sulfonate, respectively.

## 2.2 Materials Characterization

The acquired  $\text{Ni}_{0.8}\text{Co}_{0.1}\text{Mn}_{0.1}(\text{OH})_2$  particles were mixed with  $\text{LiOH}\cdot\text{H}_2\text{O}$  powders thoroughly. The mixture was first heated at 400 °C for 5h in air, and then it was cooled, removed, reground and transfer it into furnace with further calcined at 900 °C for 15 h in air to obtain  $\text{LiNi}_{0.8}\text{Co}_{0.1}\text{Mn}_{0.1}\text{O}_2$  ternary cathode composite materials which were named LAS-1 and LAS-2, LAS-3, LAS-4 according to the additive amount of sodium dodecyl benzene sulfonate, respectively.

## 2.3 Electrochemical Analysis

The electrochemical properties of  $\text{LiNi}_{0.8}\text{Co}_{0.1}\text{Mn}_{0.1}\text{O}_2$  ternary cathode prepared by CR2032 coin cell were studied. The working electrode was prepared by mixing  $\text{LiNi}_{0.8}\text{Co}_{0.1}\text{Mn}_{0.1}\text{O}_2$  ternary cathode composite with carbon black and polyvinylidene difluoride (PVDF) in N-methylpyrrolidone (NMP) at a weight ratio of 80:10:10. Using lithium metal foil as counter electrode and 1 M  $\text{LiPF}_6$  as electrolyte, the CR2032 coin battery was dissolved in a mixture of 1:1 ETH - alkylene carbonate (EC) and diethyl carbonate (DEC) by volume in Celgard separator 2340 and assembled in AR-filled gloves. All electrochemical measurements were performed at room temperature. The electro-chemical behavior of the electrodes was performed in a LAND CT-2001A system with a voltage range of 2.5 to 4.6 V vs.  $\text{Li}^+/\text{Li}$ . All electrochemical measurements were performed at room temperature. The electrochemical behavior of the electrodes was performed in a LAND CT-2001A system with a voltage range of 2.5 to 4.6 V vs.  $\text{Li}^+/\text{Li}$ .

## 3. RESULTS

The X-ray diffraction (XRD) measurement is employed to determine the crystallographic phases of the products. Figure 1 presents the XRD patterns of LAS-1 and LAS-2. The diffraction peaks located at  $2\theta = 19.98^\circ, 34.42^\circ, 39.25^\circ, 53.60^\circ, 59.72^\circ, 62.862^\circ, 79.86^\circ, \text{ and } 74.09^\circ$  correspond to (003), (101), (006), (105), (107), (018), (201), and (116) planes [30]. It could be obviously observed that all major diffraction peaks of the powder is almost consistent to the typical fingerprint of  $\text{LiNi}_{0.8}\text{Co}_{0.1}\text{Mn}_{0.1}\text{O}_2$  ternary cathode materials which belong to the layer structure of  $\alpha\text{-NaFeO}_2$ . The

sharp and well-defined diffraction peaks demonstrate the excellent nucleation and crystallization of  $\text{LiNi}_{0.8}\text{Co}_{0.1}\text{Mn}_{0.1}\text{O}_2$  ternary cathode materials during fabrication process [31]. Also, we have not observed any impurity phase. In addition, the diffraction peaks of LAS-1 is identical to LAS-2, which indicates that the crystal structure of  $\text{LiNi}_{0.8}\text{Co}_{0.1}\text{Mn}_{0.1}\text{O}_2$  ternary cathode materials did not change after the adding of LAS.

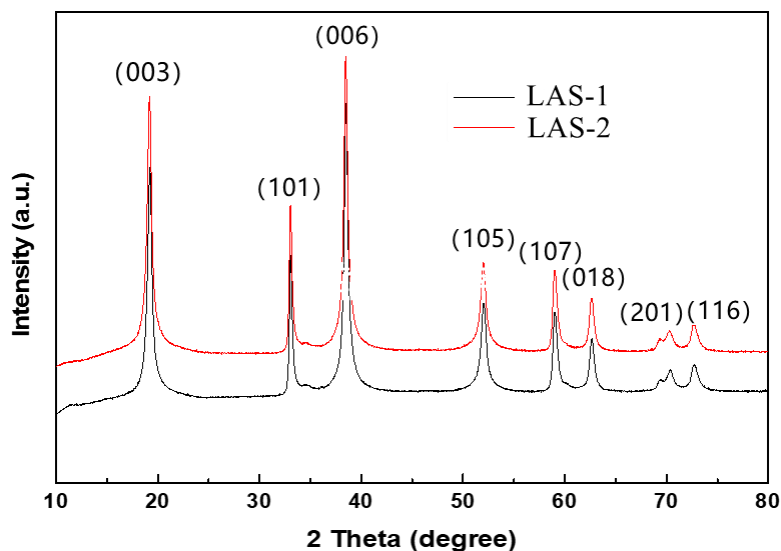


**Figure 1.** The XRD pattern of  $\text{LiNi}_{0.8}\text{Co}_{0.1}\text{Mn}_{0.1}\text{O}_2$  ternary cathode materials. The red line demonstrate the LAS assisted sample and the black line demonstrate the sample without the LAS.

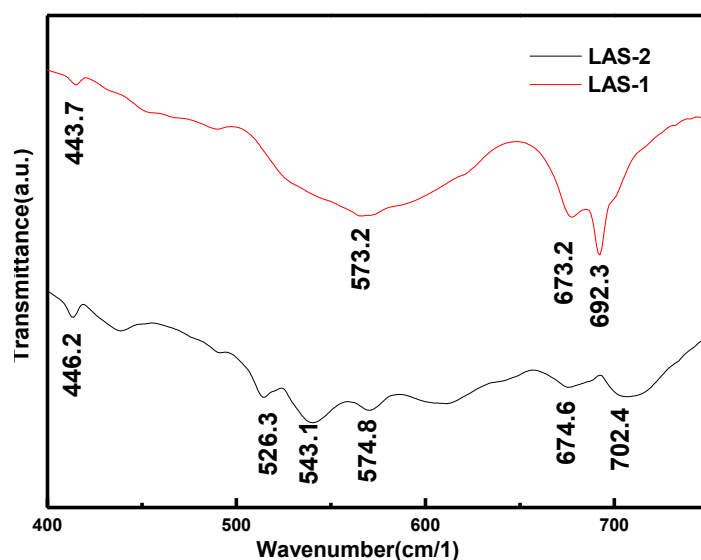


**Figure 2.** The FT-IR spectrums of the samples of LAS-1 and LAS-2.

The FT-IR has been employed to identify the chemical band of the samples as shown in Figure 2. It is obviously can be observed that the spectrum of LAS-1 is weaker than that of LAS-2 because of without adding the LAS. The absorption peaks of LAS-1 is the typical FI-IR spectrum of

$\text{LiNi}_{0.8}\text{Co}_{0.1}\text{Mn}_{0.1}\text{O}_2$  ternary material. The absorption peaks of LAS-2 is at  $446.2\text{ cm}^{-1}$ ,  $526.3\text{ cm}^{-1}$ ,  $543.1\text{ cm}^{-1}$ ,  $574.8\text{ cm}^{-1}$ ,  $674.6\text{ cm}^{-1}$  and  $702.4\text{ cm}^{-1}$ . The  $446.2\text{ cm}^{-1}$ ,  $574.8\text{ cm}^{-1}$ ,  $674.6\text{ cm}^{-1}$  and  $702.4\text{ cm}^{-1}$  are related to the vibration of Co-O, Ni-O, Mn-O, Li-O. Meanwhile, the  $526.3\text{ cm}^{-1}$ ,  $543.1\text{ cm}^{-1}$  are related to the vi-bration of  $-\text{SO}_2\text{-O}$  which indicating the introducing the LAS to the  $\text{LiNi}_{0.8}\text{Co}_{0.1}\text{Mn}_{0.1}\text{O}_2$  ternary cathode material [14, 31].

The morphology and microstructure of the as-obtained  $\text{LiNi}_{0.8}\text{Co}_{0.1}\text{Mn}_{0.1}\text{O}_2$  ternary cathode composites were investigated by means of scanning electron microscopy (SEM). As is shown in Figure 3, Figure (a, b) are the SEM images of the ternary cathode composites prepared by the precursor system without LAS, and Figure 3(c, d) are the SEM images of the ternary cathode composites prepared by precursor system with adding LAS. The shape of the LAS-1 and LAS-2 are spherical particles, and the appearance is a cluster formed by lamellar stacking, which indicating that the addition of LAS does not change the particle structure. The particle morphology of the ternary cathode material assisted by adding LAS (LAS-2) is relatively regular, and the sphereness is relatively good. The boundaries of particles are blurred and the surface is smooth without any attachment. The agglomeration degree of the particles decreases, the particles become dispersed, and the particle size distribution is more uniform [32].

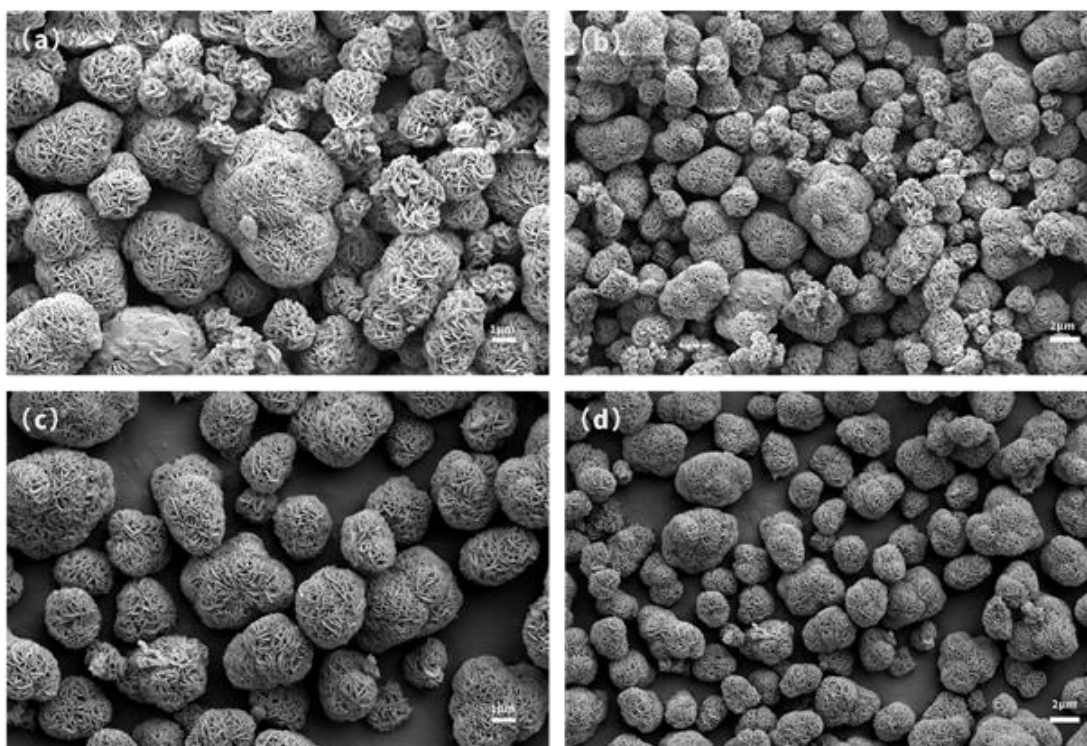


**Figure 3.** The SEM images of  $\text{LiNi}_{0.8}\text{Co}_{0.1}\text{Mn}_{0.1}\text{O}_2$  ternary cathode composites. (a, b) is the sample of LAS-1 in different magnification. (c, d) is the sample of LAS-2 in different magnification.

The electrochemical behavior of the  $\text{LiNi}_{0.8}\text{Co}_{0.1}\text{Mn}_{0.1}\text{O}_2$  ternary materials samples, as the cathode material for LIBs, was examined by LAND CT-2001A system. The initial charge-discharge

voltage profiles of the  $\text{LiNi}_{0.8}\text{Co}_{0.1}\text{Mn}_{0.1}\text{O}_2$  ternary cathode samples were tested at a current density of 200 mA/g has been shown in Figure 4 (a). The curve trend is similar, the rate of rise is fast when charging, and then the voltage steady zone slowly drops, which indicating that the addition of LAS does not hinder the removal of lithium ions [33]. The specific capacities of the four  $\text{LiNi}_{0.8}\text{Co}_{0.1}\text{Mn}_{0.1}\text{O}_2$  ternary cathode samples are obviously different, and the specific capacities of sample LAS-2 are the largest. The sample of LAS-1, LAS-2, LAS-3 and LAS-4 displayed the discharge/charge capacity are 230.9 mAh/g and 170.5mAh/g, 240.2 mAh/g and 189.5 mAh/g, 230.5 mAh/g and 164.0mAh/g, 230.3 mAh/g and 149.7mAh/g, respectively. Meanwhile, the coulombic efficiency of the four samples are 73.8%、78.9%、71.1%、65.0% in sequence. Figure 4(b) shows the cyclic performance of LAS-1, LAS-2, LAS-3 and LAS-4 at a constant current density of 200 mA/g for 50 cycles. The discharge capacity of the four samples are 165.3 mAh/g, 186.3 mAh/g, 161.1 mAh/g, 148.0 mAh/g, respectively. It is obviously found that the discharge capacity of sample of LAS-2 is higher than other three samples, which indicating that the addition of an appropriate amount of LAS is helpful to improve the discharge performance and cycle stability. At the same current density of 200  $\text{mA}\cdot\text{g}^{-1}$ , the reversible capacity of the  $\text{LiNi}_{0.8}\text{Co}_{0.1}\text{Mn}_{0.1}\text{O}_2$  ternary cathode anchored with LAS can steadily reach about 186.3 mAh/g higher than that of  $\text{LiNi}_{0.8}\text{Co}_{0.1}\text{Mn}_{0.1}\text{O}_2$  ternary composites after 50 cycles shown in Table 1.

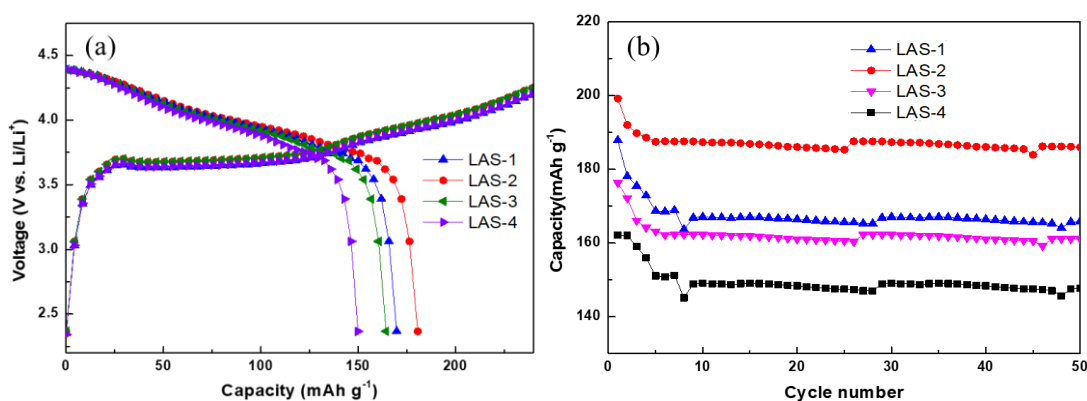


**Figure 4.** The electrochemical performance of the acquired products as the electrode for the lithium ion batteries. (a) The initial charge-discharge voltage curves of the different  $\text{LiNi}_{0.8}\text{Co}_{0.1}\text{Mn}_{0.1}\text{O}_2$  ternary cathode samples. (b) The cycle performance of the different  $\text{LiNi}_{0.8}\text{Co}_{0.1}\text{Mn}_{0.1}\text{O}_2$  ternary cathode samples.

**Table 1.** Cathode for LIBs based on  $\text{LiNi}_{0.8}\text{Co}_{0.1}\text{Mn}_{0.1}\text{O}_2$  ternary materials and their electrochemical performance.

Active Material	Current Density ( $\text{mA}\cdot\text{g}^{-1}$ )	Reversible Capacity ( $\text{mAh}\cdot\text{g}^{-1}$ )	Cycle No.	Ref.
$\text{LiNi}_{0.8}\text{Co}_{0.1}\text{Mn}_{0.1}\text{O}_2/\text{LAS}$ (our work)	200	189.5	50	
$\text{LiNi}_{0.8}\text{Co}_{0.1}\text{Mn}_{0.1}\text{O}_2/\text{LiF}$	200	171	50	34
Graphite/NMC811	200	179.8	50	35
NMC811/graphene	200	184.5	50	36

The schematic illustration of the mechanism by adding sodium dodecyl benzene sulfonate into the ternary precursors during the fabrication process shown in Figure 5. The addition of LAS to the  $\text{LiNi}_{0.8}\text{Co}_{0.1}\text{Mn}_{0.1}\text{O}_2$  ternary materials as the cathode for LIBs can optimize the morphology and electrochemical performance of terpolymer materials by forming the new chemical bonds between the metal ions on the precursor surface and the cathode group on LAS. The surfactant LAS was used to assist the precursor synthesis, and the ion pair adsorption occurred between the surface of precursor particles and the benzenesulfonic acid group which may replace other anions that may have been adsorbed on the precursor particle surface, such as  $\text{CH}_3\text{COO}^-$  [37]. LAS interacts with the metal ions of Ni, Co, Mn in the precursor by electrostatic attraction. Thus, the crystal structure and cell parameters of the material are not changed.

In preparation of ternary cathode material in the LAS auxiliary process of the precursor, the sulfo in the surfactant molecules interact with metal cation of Ni, Co, Mn and ion clusters through the electrostatic attraction, which induced orderly arrangement of metal cations [38-40]. The growth mode and rate of crystal were changed. Consequently, we get more regular crystal structure products.

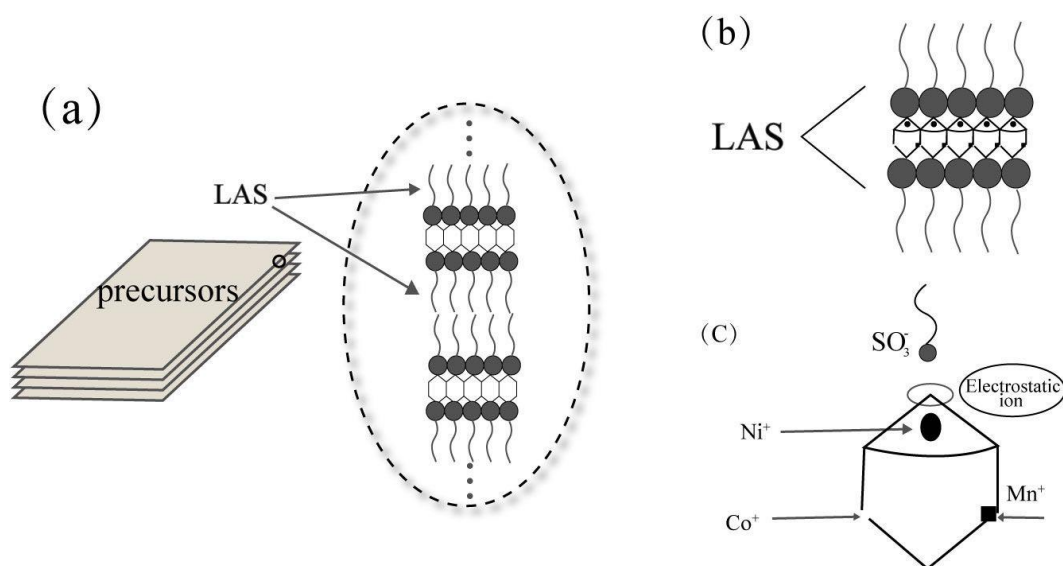


**Figure 5.** The schematic illustration of the mechanism by adding sodium dodecyl benzene sulfonate into the ternary precursors during the fabrication process.

#### 4. CONCLUSIONS

A simple method for fabricating the LAS assisted  $\text{LiNi}_{0.8}\text{Co}_{0.1}\text{Mn}_{0.1}\text{O}_2$  ternary cathode composite with excellent electrochemical performance and fine structure as the anode for LIBs has successfully developed. In this work, we use LAS as an additive to improve the layered structure of the ternary cathode materials, and make the particle distribution and size is uniform. The obtained LAS assisted  $\text{LiNi}_{0.8}\text{Co}_{0.1}\text{Mn}_{0.1}\text{O}_2$  ternary composites were utilized as the cathode for LIBs exhibited

excellent lithium storage property and enhanced cyclic performance. The LAS assisted  $\text{LiNi}_{0.8}\text{Co}_{0.1}\text{Mn}_{0.1}\text{O}_2$  ternary cathode exhibits a large discharge capacity of 240.2 mAh/g and high coulombic efficiency of 78.9% in the first cycle and displayed a capacity of 186.3 mAh/g even after 50 cycles, which indicates that LAS assisted  $\text{LiNi}_{0.8}\text{Co}_{0.1}\text{Mn}_{0.1}\text{O}_2$  ternary material has a tremendous potential as the cathode for LIBs.

#### ACKNOWLEDGMENTS

This work was supported by the financial support of the Education Scientific Research Project of Youth Teachers in the Education Department of Fujian Province (contract grant numbers JT180495), the Foundation of Science and Technology of the Sanming Institute of Fluorochemical Industry (contract grant number FCIT20171213), Fujian Key Project of Science and Technology (contract grant number 2121G02012), University Industry Research Cooperation Project of Fujian (contract grant number 2022H6035) and the Scientific Research Foundation for Introducing Talent of Sanming University (contract grant numbers KD180017).

#### References

1. R.Jung, R. Morasch, P. Karayaylali, K. Phillips, F. Maglia, C. Stinner, Y. Shao-Horn, H.A. Gasteiger, *Journal of Electrochemical Society*, 165(2018)132.
2. C. Busà, M. Belekoukia, Loveridge, M, *Electrochimical Acta*, 366(2021)137358.
3. O. Dolotkoab, A. Senyshynb, M.J. Mühlbauerabc, K. Nikolowskiac, H. Ehrenberg, *Journal of Power Source*, 255(2014)197.
4. X . Bai, R. He, A . Wei, X. Li, Z. Liu, *Journal of Alloys and Compounds*, 857(2021)157877.
5. T . Ryoichi, Y. Yang, K. Pinar, *ACS Applied Materials & Interfaces*, 11(2019) 34973.
6. X . Dong, J . Yao, W. Zhu, ; X. Huang, X. Kuai, J . Tang, X. Li, S. Dai, L. Shen, R. Yang, *Journal of Materials Chemistry A*, 7(2019) 20262.
7. M. Du, P. Yang, W. He, S. Bie, J. Liu, *Journal of Alloys and Compounds*, 805(2019)991.
8. L. Song, A. Li, Z. Xiao, Z. Chi, H. Zhu, *Ionics*, 26(2020) 2681.
9. A. Ghosh, J.M. Foster, G.J. Offer, M. Marinescu, *Journal of Electrochemical Society*, 168(2021)020509.
10. R.C. Lee, J. Franklin, C. Tian, D. Nordlund, R. Kostecki, *Journal of Power Source*, 498(2021)229885.
11. Y. Yang, P. Karayaylali, L. Giordano, J. Corchado-García, S.H. Yang, *ACS Applied Materials & Interfaces*, 12(2020) 55865.
12. J. Zhang, Q. Wang, S. Li, Z. Jiang, S. Tan, X. Wang, K. Zhang, Q. Yuan, S.J. Lee, C.J. Titus, *Nature Communication*, 11(2020)6342.
13. M. Beak, J. Park, S. Park, S. Jeong, J. Kang, W. Choi, W.S. Yoon, K. Kwon, *Journal of Hazardous Materials*, 425 (2022) 127907.
14. G. Chen, B. Peng, R. Han, N. Chen, Q. Wang, *Ceramics International*, 46(2020) 20985.
15. M. Woodcox, R. Shepard, M. Smeu, *Journal of Power Source*, 516(2021) 230620.
16. J.R. Croy, A. Gutierrez,; M. He, B.T. Yonemoto, E. Lee, M.M. Thackeray, *Journal of Power Source*, 15 (2019) 226706.
17. T. Wang, K. Ren, W. Xiao, W. Dong, H. Wang, *Journal of Materials Chemistry C*, 124 (2020) 5600.
18. C.Y. Wu, Q. Bao, Y.T. Tsai, J.G. Duh, *Journal of Alloys and Compounds*, 865(2021)158806.
19. Z. Chen, H. Nguyen, M. Zarrabeitia, H. Liang, D. Bresser, *Advanced Functional Materials*, 31(2021) 2105343.
20. R. Li, Y. Ming, W. Xiang, C.L. Xu, G.L. Feng, *RSC Advance*, 9(2019)36849.
21. Y. Feng, H. Xu, B. Wang, S. Wang, S. Li, *Journal of Electrochemical Energy Conversion and*



- Storage*, 18(2021)031005.
22. X. Xiong, Z. Wang, X. Yin, H. Guo, X. Li, *Materials Letters*, 110(2013)4.
  23. R.P. Guo, J.Z. Kong, P. Xu, *Ionics*, 27(2021)5009.
  24. H. Zhang, J. Xu, J. Zhang, *Frontiers of Materials Science*, 309(2019).
  25. X. Zheng, X. Li, Z. Bao, Z. Wang, X. Yan, *Ceramics International*, 42(2016)644.
  26. F. Xiong, Z. Chen, C. Huang, T. Wang, F. Chen, *Inorganic Chemistry*, 58(2019)15498.
  27. M. Zhang, H. Zhao, M. Tan, J. Liu, Y. Hu, S. Liu, X. Shu, H. Li, J. Cai, *Journal of Alloys and Compounds*, 774(2019)82.
  28. Z.L. Xiao, C.F. Zhou, L.B. Song, Z. Cao, P. Jiang, *Ionics*, 27(2011)1909.
  29. J.W. Li, Y. Li, W.T. Yi, P.H. Ma, *Journal of Materials Science-Materials Electronics*, 30(2019) 7490.
  30. M. Zhao, Y. Xu, P. Ren, Y. Zuo, W. Su, Y.F. Tang, *Dalton Transactions*. 49(2020) 2933.
  31. J. Dong, H.H. He, D.Y. Zhang, C. Chang, *Journal Materials Science-Materials Electronics*, 30(2019)18200.
  32. L.W. Liang, G.R. Jiang, *Journal of Alloys and Compounds*, 657(2016)570.
  33. C. Xu, K. Mrker, J. Lee, A. Mahadevegowda, C.P. Grey, *Nature Materials*, 20(2021)84.
  34. X.H. X, Z.X. Wang, X. Yin, H.J. Guo, X.H. Li, *Materials Letters*, 110(2013)4.
  35. K. Marker, C. Xu, C.P. Grey, *Journal of the American Chemical Society*, 142(2020) 17447.
  36. S. Jan, S. Nurgul, X.Q. Shi, H. Xia, H. Pang, *Electrochimica Acta*, 149(2014)86
  37. K. Mrker, ; P.J. Reeves, C. Xu, K.J. Griffith, C.P. Grey, *Chemistry of Materials*, 31(2019) 2545.
  38. L. Tang, X. Cheng, R. Wu, T. Cao, Z. Zhang, *Journal Of Energy Chemistry*, 66(2022)9.
  39. F. Xin, H. Zhou, X. Chen, M. Zuba, M.S. Whittingham, *ACS Applied Materials & Interfaces*, 11 (2019) 34889.
  40. S.P. Ma, X.Q. Zhang, S.M. Li, Y.X. Cui, Y.H. Cu, *Ionics*, 26 (2020) 2165.